JOURNAL OF THERMOPHYSICS AND HEAT TRANSFER
Vol. 9, No. 1, January–March 1995

Thermal Contact Resistance Between Balls and Rings of a Bearing Under Axial, Radial, and Combined Loads

Katsuhiko Nakajima*
NTT Radio Communication Systems Laboratories, Yokosuka 238-03, Japan

The thermal contact resistance between the balls and the inner and outer rings of a space-use deep groove ball bearing is investigated assuming that heat transfer between smooth contacting elements occurs through the elastic contact areas. It is also assumed that the stationary bearing sustains axial, radial, or combined loads under a steady-state temperature condition. The shapes and sizes of the contact areas are calculated using the Hertzian theory. In particular, the contact force for the axial load is determined with careful consideration of the change in the contact angle induced by elastic deformation at the contact area. The correlation between the experimental data and the calculated values confirms the validity of the prediction method for the thermal contact resistances between the elements of a dry bearing with a surface roughness of less than 0.5×10^{-6} m under the mean temperature of less than 353 K, and temperature differences across the rings of less than 35 K.

Nomenclature

A, B	=	parameters given by Eq. (2), 1/m
a, b	=	semimajor and -minor axes of contact ellipse, m
C	=	parameters given by Eq. (12b)
D	=	parameters given by Eq. (10b), m/Pa
E	=	modulus of elasticity, Pa
e	=	eccentricity of contact ellipse
F_a, F_r	=	axial and radial loads, respectively, N
g_r	=	radial clearance of bearing, m
$K_1(e, \pi/2)$	=	complete elliptic integral of the first kind
$K_2(e, \pi/2)$	=	complete elliptic integral of the second kind
k	=	thermal conductivity, W/mK
m, n	=	shape parameters of contact ellipse
N	=	number of balls in bearing
P	=	contact force, N
Q	=	heat flow, W
R	=	thermal resistance, K/W
r, r'	=	radii of curvature for race and groove, respectively, m
T	=	temperature, K
X, Y	=	coefficient of static equivalent radial and axial loads, respectively
β	=	contact angle of bearing, rad
γ	=	included angle between radial load component and combined load shown in Fig. 3, rad
δ	=	sum of displacements of two contacting solids, m
θ	=	angle between adjacent two balls of bearing, rad
λ	=	coefficient of thermal expansion, m/mK
ν	=	Poisson's ratio
σ	=	Stefan-Boltzmann constant, 5.67×10^{-8} W/m^{2}K^4

Subscripts

b	=	ball or ball side of bearing
i	=	inner ring or inner ring side of bearing
o	=	outer ring or outer ring side of bearing

Introduction

LARGE satellite onboard antennas are being developed for multibeam satellite communication systems.[1] The beam-pointing accuracies required of multibeam antennas are stringent, and sophisticated deployment techniques are needed in order to meet the limited stowage diameters of the launch vehicles. To achieve the high beam pointing accuracies required, the thermal distortion of bearings used in the deployment mechanisms must be minimized by controlling not only the temperatures within the allowable ranges for the units, but also the temperature differences between the inner and the outer rings within the design ranges.[2–4]

The configuration of the ball bearings dealt with in this article is schematically shown in Fig. 1. The temperature differences across the ball bearings of the antenna deployment mechanisms are generally controlled by using multilayer insulation and electric heaters. The thermal control subsystem must be designed considering heat transfer in the radial direction such as conduction through the inner ring, the outer ring and the balls, conduction through contacting interfaces between the elements, and radiation interchange between the elements. For instance, the author has estimated the magnitudes of the thermal resistances corresponding to the above heat transfer modes from the results of thermal balance tests of an antenna that had deployment mechanisms that used deep groove ball bearings.[4] The values were about 2.3 K/W

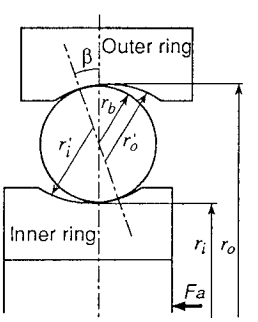

Fig. 1 Schematic of bearing.

Received July 9, 1992; revision received April 2, 1994; accepted for publication June 7, 1994.

*Senior Research Engineer, Supervisor, Satellite Communication Systems Laboratory. Member AIAA.

in total for conduction through the elements, and about 2.2 K/W in total for conduction through the contacting interfaces between the bearing and the shaft/housing. The contact resistance was about 35 K/W for the interfaces between the balls and the inner/outer rings. The radiation resistance was small enough to neglect at the temperature of 283 K. With respect to these thermal resistances, the values for conduction through the bearing elements themselves and for radiation can be calculated using the dimensions, the thermal conductivities, the thermo-optical properties, and the temperatures of the elements. However, it can be said that the thermal contact resistances between the balls and the rings, which are most closely related to the temperature differences across the bearings, are difficult to predict because no useful calculation methods have been proposed yet.

Since the thermal resistance results from the fact that most of the heat is constrained to flow through small contact areas, a reasonable step in determining the contact resistance between the balls and the inner and outer rings of the bearing would be to use a similar approach to that adopted to solve the thermal constriction problem for ideal smooth surfaces. The thermal constriction resistances for circular, circular annular, rectangular, and other geometrical-shaped contact areas are normally solved analytically or numerically as Dirichlet problems.[5-7] The prediction of the thermal contact resistance necessitates the determination of the contact area. This is possible with the Hertzian theory when the contact surfaces are approximated as being smooth. In addition to the study by Clausing and Chao,[8] the thermal contact resistance problem has been discussed in many papers.[9,10] Most papers determine the contact areas using the Hertzian theory. However, a survey of the literature shows that only the studies by Yovanovich[11-13] have dealt with the problem of the contact resistance between bearing elements. He studied the contact resistance under axial loads and concluded that the contact resistance depends on the size and shape of contact area as determined by the Hertzian theory and the thermal conductivity of the material. He did not, however, give thermal designers a tractable expression that considered the change in contact angle induced by elastic deformation at the contact points. Also, he did not consider other types of loadings such as radial and combined axial/radial loads.

This article develops an approach that accurately predicts the thermal contact resistance between the balls and the inner and outer rings of a space-use deep groove ball bearing with solid lubricant. This is quite valuable because the suppression of thermal distortion is essential to realize deployable multibeam satellite antennas that have high beam pointing accuracies. The analysis assumes that the temperature of the bearing is steady. We note that the thermal contact resistance discussed in this article is based on the macroscopic contact area determined with the Hertzian theory, and the effect of surface roughness or waviness is neglected. This is reasonable because the surface roughness of the bearings treated in this study is less than 0.5×10^{-6} m, and for such smooth surfaces it has been shown that the total contact resistance can be discussed by considering just the macroscopic contact area.[8,12] The contact forces required to calculate the contact area are explicitly formulated for axial, radial, and combined loadings. In particular, an expression for the axial load is derived by carefully considering the change in contact angle induced by elastic deformation at the contact area. The prediction method for the thermal contact resistance is verified by comparing the calculated values with experimental results measured in a vacuum environment.

Expressions for Contact Resistance

Contact Area of Elastic Bodies

The thermal contact resistance is generally considered as a function of the shape and size of the contact area. This area becomes elliptic when two elastic bodies having smooth round surfaces are pressed against each other. The formulations that determine the semimajor and -minor axes of the elliptic contact area are summarized herein.[14-17] In deriving the following expressions, it is assumed that the angle between the two planes containing the principal radii of curvature of the bodies are perpendicular as in the case of balls contacting the inner or outer ring of a bearing:

$$a = m\left[\frac{3\pi}{4}\frac{P}{A+B}\left(\frac{1-\nu_1^2}{\pi E_1}+\frac{1-\nu_2^2}{\pi E_2}\right)\right]^{1/3} \tag{1a}$$

$$b = n\left[\frac{3\pi}{4}\frac{P}{A+B}\left(\frac{1-\nu_1^2}{\pi E_1}+\frac{1-\nu_2^2}{\pi E_2}\right)\right]^{1/3} \tag{1b}$$

$$A+B=\frac{1}{2}\left(\frac{1}{r_1}+\frac{1}{r_1'}+\frac{1}{r_2}+\frac{1}{r_2'}\right),\quad \frac{A}{B}=\frac{1/r_1+1/r_2}{1/r_1'+1/r_2'} \tag{2}$$

The values of m and n are calculated by the following equations[15-17]:

$$m=\left(\frac{I+J}{\pi}\right)^{1/3},\qquad n=m(1-e^2)^{1/2} \tag{3a}$$

$$e=[1-(b/a)^2]^{1/2},\qquad \frac{A}{B}=\frac{J}{I} \tag{3b}$$

$$I=\frac{2}{e^2}\left[K_1\left(e,\frac{\pi}{2}\right)-K_2\left(e,\frac{\pi}{2}\right)\right]$$

$$J=\frac{2}{e^2}\left[\frac{K_2(e,\pi/2)}{1-e^2}-K_1\left(e,\frac{\pi}{2}\right)\right] \tag{3c}$$

$$K_1\left(e,\frac{\pi}{2}\right)=\frac{\pi}{2}\left\{1+\left(\frac{1}{2}\right)^2e^2+\left(\frac{1\cdot3}{2\cdot4}\right)^2e^4+\cdots+\left[\frac{(2n-1)(2n-3)\cdots3\cdot1}{2n(2n-2)\cdots4\cdot2}\right]^2e^{2n}\right\} \tag{3d}$$

$$K_2\left(e,\frac{\pi}{2}\right)=\frac{\pi}{2}\left\{1-\left(\frac{1}{2}\right)^2e^2-\left(\frac{1\cdot3}{2\cdot4}\right)^2\frac{e^4}{3}-\cdots-\left[\frac{(2n-1)(2n-3)\cdots3\cdot1}{2n(2n-2)\cdots4\cdot2}\right]^2\frac{e^{2n}}{2n-1}\right\} \tag{3e}$$

Also, the sum of the displacements of two bodies against the contacting surface is given by[15]

$$\delta=\frac{2K_1(e,\pi/2)}{m\pi}\left[\left(\frac{3\pi}{4}\right)^2P^2(A+B)\times\left(\frac{1-\nu_1^2}{\pi E_1}+\frac{1-\nu_2^2}{\pi E_2}\right)^2\right]^{1/3} \tag{4}$$

Let us consider the bearing model shown in Fig. 1. For the contact at the inner ring side, the radius of curvature r_i' of the inner groove must be treated as negative in Eq. (2). Also, r_o and r_o' must be treated as negative at the outer ring side contact.

Contact Resistance

The contact resistances between the balls and the inner and outer rings may be treated in the same manner as constriction resistance since both resistances result from the restriction of the heat flow due to small contact areas. Thus, the assumptions utilized to solve the constriction resistance may be applicable to the present problem, whereas a numerical verification must be performed for the bearing dealt with in this study. The assumptions are as follows:

1) The dominant heat flow is conduction through the contact area, i.e., the effect of radiation is neglected because the temperature of each bearing element is not high.

2) The heat flow pattern in both elements is approximated as symmetric about the contact area, and thus the contact area is isothermal.

3) Based on the above, the temperatures at points far from the contact area can be treated as being constant.

The boundary problem of Laplace's equation for the elliptic contact area can be solved by using the ellipsoidal coordinate system instead of the Cartesian system under the boundary conditions: 1) $T = T_0 = \text{const}$ at the contact plane, and 2) $T = 0$ at the points far from the contact plane.[5-7,12] Thus, the temperature distribution in the conducting half-space is given by[12]

$$\frac{T}{T_0} = \int_u^\infty \phi^{-1/2}(u)\,du \Big/ \int_0^\infty \phi^{-1/2}(u)\,du$$
$$\phi(u) = (a^2 + u)(b^2 + u)u \tag{5}$$

where u is the variable along an axis normal to the contact plane. Furthermore, at points sufficiently far from the contact area, the heat flow is approximately radial and can be written as[12]

$$q_r = \frac{Q}{2\pi r^2} \cong 2kT_0 \Big/ r^2 \int_0^\infty \phi^{-1/2}(u)\,du \tag{6}$$

where Q is all the heat leaving the elliptic contact area, k is the thermal conductivity of the conducting half-space, and r is the distance from the center of the elliptic contact area.

From Eqs. (5) and (6), the thermal contact resistance is written as

$$R = \frac{T_0 - T_{u\to\infty}}{Q} = \frac{1}{4\pi k}\int_0^\infty [(a^2 + u)(b^2 + u)u]^{-1/2}\,du \tag{7}$$

Using the complete elliptic integral of the first kind, Eq. (7) can be rewritten in the following form as[12,13]

$$R = \frac{\Psi(a/b)}{4ka}, \qquad \Psi(a/b) = \frac{2}{\pi}K_1\left(e, \frac{\pi}{2}\right) \tag{8}$$

Then, the contact resistance between the ball and the inner or outer ring can be determined by using Eq. (8). For most bearings, whose balls and both rings are made from the same material, i.e., $k = k_b = k_i = k_o$, we can write the contact resistance per ball as

$$R = \frac{1}{2k}\left[\frac{\Psi(a_i/b_i)}{a_i} + \frac{\Psi(a_o/b_o)}{a_o}\right] \tag{9}$$

or

$$R = \frac{1}{2kP^{1/3}}\left[\frac{\Psi(m_i/n_i)}{m_i(3\pi D_i/4)^{1/3}} + \frac{\Psi(m_o/n_o)}{m_o(3\pi D_o/4)^{1/3}}\right] \tag{10a}$$

$$D_i = \frac{2}{A_i + B_i}\left(\frac{1-\nu^2}{\pi E}\right), \quad D_o = \frac{2}{A_o + B_o}\left(\frac{1-\nu^2}{\pi E}\right) \tag{10b}$$

$$\Psi(m_i/n_i) = \frac{2}{\pi}K_1\left(e_i, \frac{\pi}{2}\right), \quad \Psi(m_o/n_o) = \frac{2}{\pi}K_1\left(e_o, \frac{\pi}{2}\right) \tag{10c}$$

where the relation $a/b = m/n$ is used, and $\Psi(a/b) = \Psi(m/n)$ is frequently called the constriction parameter. These expressions permit us to predict the total contact resistance resulting from the contact of an arbitrary number of balls with both the inner and outer rings by connecting the thermal resistances in parallel.

Load Types and Contact Forces

We can now use Eqs. (8), (9), or (10) for the prediction of the contact resistance if the contact force for each ball is determined from the total load on the bearing. The contact force is then formulated assuming that the balls and both the inner and outer rings are made from the same material, and that the bearing has a positive radial clearance.

Contact Forces Under Axial Loads

All the contact forces become equal when the bearing sustains an axial load (see Fig. 1). Considering the contact angle the contact force is given by

$$P = \frac{F_a}{N\sin\beta}, \qquad \cos\beta = \frac{r_i' + r_o' - 2r_b - g_r/2}{r_i' + r_o' - 2r_b + \delta/2} \tag{11}$$

where β must be calculated taking into account the elastic deformations at the inner and outer ring contact points. Based on Eq. (4), the deformation δ in Eq. (11) is given by

$$\delta = \left[\frac{2\cos\beta_2}{\pi N}\left(\frac{F_a}{\sin\beta}\right)^{2/3}\frac{1-\nu^2}{E}\right] \times \left[C_i\left(\frac{N}{D_i}\right)^{1/3} + C_o\left(\frac{N}{D_o}\right)^{1/3}\right] \tag{12a}$$

$$C_i = \frac{2K_1(e_i, \pi/2)}{m_i\pi}\left(\frac{3\pi}{4}\right)^{2/3}, \qquad C_o = \frac{2K_1(e_o, \pi/2)}{m_o\pi}\left(\frac{3\pi}{4}\right)^{2/3} \tag{12b}$$

where D_i and D_o are given by Eq. (10b). The parameters C_i, C_o, D_i, and D_o must be calculated using the radii of curvature given by

$$r_{i\beta} = r_i + r_i'(1 - \cos\beta), \qquad r_{o\beta} = r_o - r_o'(1 - \cos\beta) \tag{12c}$$

Thus, β and the contact force for each ball can be determined by solving Eqs. (11) and (12a–12c) numerically as simultaneous equations.

Furthermore, by substituting Eq. (11) into Eq. (10a), and considering the number of contacting balls, the explicit representation for the total contact resistance under axial load is given as

$$R = \frac{1}{2kN^{2/3}}\left(\frac{F_a}{\sin\beta}\right)^{-1/3}\left[\frac{\Psi(m_i/n_i)}{m_i(3\pi D_i/4)^{1/3}} + \frac{\Psi(m_o/n_o)}{m_o(3\pi D_o/4)^{1/3}}\right] \tag{13}$$

Contact Forces under Radial Loads

The representative relation between the radial load and the locations of balls is shown in Figs. 2a and 2b. The contact force on each ball in both cases is determined from the equilibrium condition of the total radial load and the contact forces based on Eq. (4). The contact forces in the case of Fig. 2a are given by

$$F_r = P_0(1 + 2\cos^{5/2}\theta + 2\cos^{5/2}2\theta + \ldots + 2\cos^{5/2} j\theta)$$
$$j = 1, 2, \cdots \tag{14a}$$

$$P_1 = P_0\cos^{3/2}\theta,\ P_2 = P_0\cos^{3/2}2\theta,\ \ldots,\ P_j = P_0\cos^{3/2}j\theta \tag{14b}$$

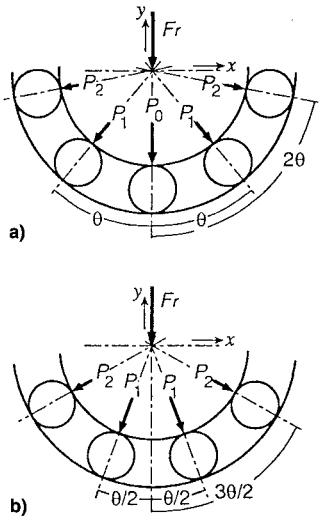

Fig. 2 Radial load and ball positions.

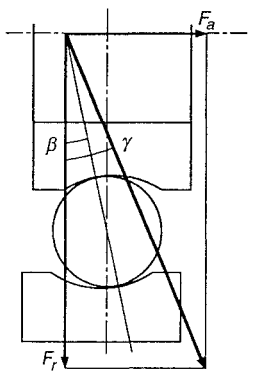

Fig. 3 Included angle γ between radial load component and combined load.

The contact forces in the case of Fig. 2b are given by

$$F_r = 2P_1\left[\cos\frac{\theta}{2} + \cdots + \cos^{3/2}(j-1)\theta\cos\frac{(2j-1)\theta}{2}\right] \quad j = 1, 2, \ldots \tag{15a}$$

$$P_2 = P_1\cos^{3/2}\theta, \ldots, P_j = P_1\cos^{3/2}(j-1)\theta \tag{15b}$$

Here we note that the balls sustaining the radial load are restricted to those located within $j\theta \leq \pi/2$, since positive radial clearance is assumed in this study. We can now calculate each contact resistance individually by using Eqs. (10) and (14) or (15), and the total resistance is predicted by connecting the resistances in parallel.

Contact Forces Under Combined Loads

The combined load of the axial and the radial loads are commonly approximated by the static equivalent load F_e as

$$F_e = XF_r + YF_a, \quad (F_a \geq \alpha F_r) \tag{16a}$$

$$F_e = F_r, \quad (F_a < \alpha F_r) \tag{16b}$$

where X, Y, and the value of α are inherent bearing parameters. In the case of Eq. (16a), the contact forces on the balls are calculated in much the same way as for axial loading.

However, even if the condition for Eq. (16b) is satisfied, we must determine if β of the bearing is larger than γ between the radial load component and the combined load (see Fig. 3), because Eq. (16b) is an approximation that is applicable only when the included angle is less than the contact angle. This means that we must consider the contacts induced by the axial load component even for the balls that are located at positions larger than $j\theta > \pi/2$, i.e., above the x axis in Figs. 2a or 2b, when the included angle is larger than the contact angle, in addition to the contacts caused by combined load for the balls located below the x axis. The contact forces for the balls above the x axis are calculated in the same manner as for the axial load, whereas the balls below the x axis are handled in the same manner as for the radial load.

To recapitulate, we can calculate the contact force in the same way as in the case of radial load only when the included angle between the radial load component and the combined load is smaller than the contact angle of the bearing.

Applicability of Assumptions

For the single row dry bearing, the thermal contact resistances under axial loads were calculated in order to verify the adequacy of the fundamental assumptions used to derive the formula for the contact resistance. The bearing includes seven spherical balls, and all elements were made from stainless steel 440C. The diameter of balls, $2r_b$, was 9.525×10^{-3} m. The groove radii r_i' and r_o' were $1.03937r_b$, and the race radii r_i and r_o were $3.06037r_b$ and $5.06562r_b$, respectively. The inner and the outer bearing diameters were 22×10^{-3} m and 56×10^{-3} m, and the width was 16×10^{-3} m. The surface of each contacting element was coated with MoS_2 lubricant, and the roughness was less than 0.5×10^{-6} m.

In the numerical calculations, which were performed considering the temperature difference between the inner and the outer rings, the resistance for the conduction through each MoS_2 layer was neglected because the estimated value of 0.3 K/W was sufficiently small compared to the contact resistance of about 35 K/W. Also, only thermal expansion in the radial direction was considered for all elements, since this had the greatest effect upon the geometrical shapes and sizes of the contact areas. The following material properties were used for the calculation; the modulus of elasticity was 200 GPa, Poisson's ratio was 0.25, the coefficient of thermal expansion

Table 1 Parameters of thermal contact resistance

	Inner ring/ball	Outer ring/ball
T, K	273/288	303/288
A/B	35.0	21.2
m	3.95	3.23
m/n	9.75	7.13
a/b	0.309/0.0317	0.295/0.0414
$K_1(e, \pi/2)$	3.67	3.36
$\Psi(a/b)$	2.34	2.14

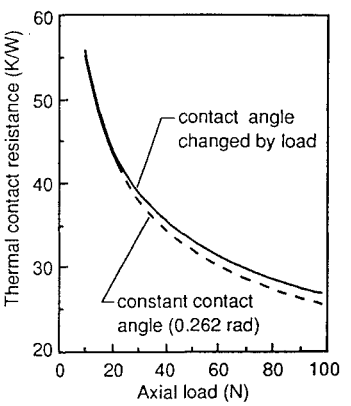

Fig. 4 Effect of contact angle change upon the thermal contact resistance.

was 10.3×10^{-6} K^{-1}, and the thermal conductivity was 23.8 W/mK. The temperatures of the inner and the outer rings were taken as being 273 and 303 K, respectively. The parameters relating to the contact resistance are shown in Table 1. The variation of the contact resistance against the axial load is shown in Fig. 4. The solid line shows the resistance that was obtained considering the change in the contact angle and the radii of curvature r_i, r_o, and r_b, which were obtained by

$$r_i = r_{ir}[1 + \lambda(T_{ic} - T_r)] \tag{17a}$$

$$r_o = r_{or}[1 + \lambda(T_{oe} - T_r)] \tag{17b}$$

$$r_b = r_{br}[1 + 2\lambda(T_{be} - T_r)] \tag{17c}$$

where r_{ir}, r_{or}, and r_{br} are the radii at the reference temperature T_r, 293 K. T_{ic}, T_{oc}, and T_{be} are the temperatures of the inner ring, the outer ring, and the balls, respectively. Here, using the constriction parameter ratios for the inner and the outer ring side contacts, the temperatures of the balls were calculated by

$$T_{be} = 0.478T_{ic} + 0.522T_{oe} \tag{18}$$

The dotted line shows the result when the change in the contact angle was neglected by using the nominal value of 0.262 rad. These results reveal that special attention must be paid to changes in the contact angle to accurately predict the contact resistance between the balls and the inner and outer rings.

Effect of Radiation Interchange

The validity of neglecting radiation interchange between the bearing elements was verified by estimating its effect on the contact resistance shown by the solid line in Fig. 4. Let us put the resistances for a direct radiation interchange between the inner and the outer rings as R_{r1}, and for the interchange between both rings via the balls as R_{r2}. These resistances are represented as

$$R_{r1} = \frac{1}{\varepsilon_o S_o F_{oi} \varepsilon_i \sigma (T_o^2 + T_i^2)(T_o + T_i)} \tag{19a}$$

$$R_{r2} = \frac{1}{2\varepsilon_o S_o F_{ob} \varepsilon_b \sigma} \left(\frac{2}{T_o + T_i}\right)^3 \tag{19b}$$

where F, S, and ε denote the configuration factor, the surface area and the emissivity, respectively. The resistances of R_{r1} = 3540 K/W and R_{r2} = 18,400 K/W were obtained by numerical calculation, using the bearing dimension and the emissivities of $\varepsilon_b = \varepsilon_i = \varepsilon_o = 0.8$. This unmeasured value of emissivity was used in order to avoid underestimating the effect. The total radiation resistance—both resistances connected in parallel—became 2970 K/W. The effect of this resistance upon the values shown in Fig. 4 was less than 1%, and so is almost negligible from an engineering point of view.

In addition, if the effect of 2% for the contact resistance is allowable, we can neglect the radiation interchange when the mean temperature of the bearing is below 353 K and the temperature difference between both rings is within 35 K. Actual antenna deployment mechanisms[4] use thermal control for the bearings so as to keep the temperature difference between both rings below 30 K, and the mean temperature within 183–343 K. Therefore, it can be concluded that the assumptions used in the thermal analysis of the contact resistance are valid provided the temperature conditions mentioned above are satisfied.

Convergence of Temperature Gradient

The contact resistance was formulated assuming that the heat flow pattern is uniform and the temperature converges to a constant value at points sufficiently far from the contact area. If this assumption is applicable to the contact resistance problem of the bearing elements, the integral term of Eq. (7) corresponding to the temperature variation must tend towards a constant value, or the gradient obtained from the differential of Eq. (7) must approximate zero within the dimensions of the inner and the outer rings.

Thus, the numerical calculation of the differential of Eq. (7) was performed while omitting the constant and sign, and taking u as a variable that corresponds to the distance from the contact area. Figure 5 shows the typical results regarding the bearing under discussion. The curves for a/b = 9.75 and 7.13 correspond to the contacts at the inner ring and the outer ring sides, respectively. The radii of semiminor axis at the inner ring side contact area are 31.7×10^{-6} m and 54.3×10^{-6} m under the axial loads of 18.5 N and 98.1 N, respectively. In the case of $b = 31.7 \times 10^{-6}$ m, the region of $u/b < 170$ corresponds to the inside of the inner ring, whereas in the case of $b = 54.3 \times 10^{-6}$ m, the region of $u/b < 100$ is the inside of the inner ring. Therefore, Fig. 5 leads to the conclusion that the assumption adopted for the temperature distribution is appropriate to the contact-resistance problem of the bearing in this study.

Experimental Results and Comparison with Theoretical Prediction

Experiment

A test program was conducted in order to verify the prediction method of the thermal contact resistance. The dimensions and material properties of the bearing matched those described previously. The experimental apparatus consisted of a vacuum chamber equipped with vacuum pumps and liquid nitrogen cooled shrouds, and a temperature measurement instrument using thermocouples as sensors. The bearing was assembled on a shaft and a cylindrical housing, both of which were made from stainless steel 304. The mass of the shaft was 0.55 kg. The interfaces between the inner ring and the shaft as well as the outer ring and the housing were coated with silicone thermal compound to enhance the heat transfer be-

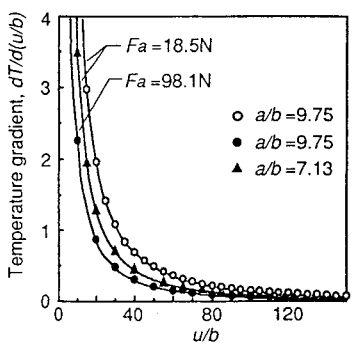

Fig. 5 Convergence characteristics of temperature gradients.

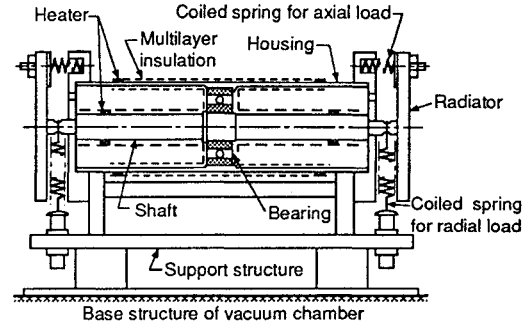

Fig. 6 Experimental setup for thermal contact resistance measurement.

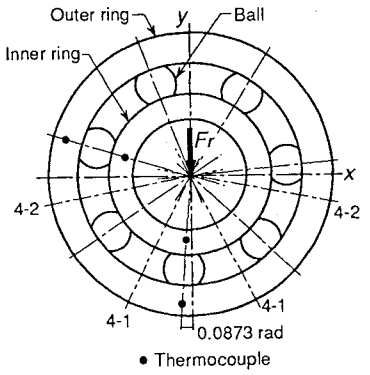

Fig. 7 Temperature measurement points on bearing.

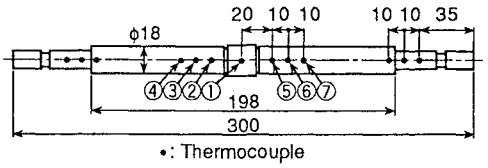

Fig. 8 Temperature measurement points on shaft.

tween them. This assembly was supported by a structure fitted with loading springs, as shown in Fig. 6. Based on the calibrated force vs displacement relationships, the axial load was equally imposed by adjusting the displacements of the three springs fitted to each side while the radial load was imposed by two springs. Figures 7 and 8 show the temperature measurement points on the bearing and the shaft.

The tests were performed in a vacuum environment at pressures lower than 1.33×10^{-3} Pa, and the shroud temperatures were under 100 K. The test parameters were shown in Table 2. The temperatures shown in Table 2 were obtained under steady-state conditions when temperature changes of ± 0.1 K were kept for at least 1 h.

Experimental Results

The heat flow through the shaft was considered to be identical with the heat flow across the inner and the outer rings, due to the fact that the temperature gradients were fairly constant on both sides of the shaft. The conductive heat flow through the shaft Q was calculated by

$$Q = S_s k_s \left(\frac{T_2 - T_4}{l_{24}} + \frac{T_5 - T_7}{l_{57}} \right) \tag{20}$$

where T_2, T_4, T_5, and T_7 are the temperatures at measurement points shown in Fig. 8. The distances between points ② and ④, and ⑤ and ⑦ are denoted as l_{24} and l_{57}. Also, the sectional area and the thermal conductivity of the shaft are represented by S_s and k_s, respectively. Thus, the contact resistance R_e between the ball and the inner and the outer rings was calculated as follows:

$$R_e = \frac{|T_i - T_o|}{Q} - R_s = R_{io} - R_s \tag{21}$$

where T_i, T_o, and R_s denote the measured temperatures of the inner and the outer rings, and the conductive resistance for the solids existing between these temperature measurement points.

The test results of contact resistance are summarized in Table 3. These results include the experimental uncertainty stated below. To calculate the resistances, the thermal conductivity of the shaft was taken as 15.5 W/mK at the temperature of 268 K, which was the mean value for all experimental cases. This value of thermal conductivity was applied to all test cases because the consideration of the individual mean temperature for each test case yielded a maximum relative difference of $\pm 0.4\%$ in the thermal resistance. Uncertainty is also created by the temperature stability at the measuring points on the shaft; the temperature fluctuation of ± 0.1 K changed the thermal contact resistance by $\pm 5.0\%$. The other uncertainty factor was the accuracy of the load, $\pm 1.3\%$, due to the temperature dependency of the force vs displacement relationships of the springs. Consequently, the total experimental uncertainty was estimated to be $\pm 6.7\%$ by using the linear summation method, whereas the rms method resulted in a value of less than $\pm 5.2\%$.

Table 2 Experimental cases and parameters

Test case no.	Load, N		Mean temperature, K	
	Axial	Radial	Inner ring	Outer ring
1	39.2	0	268.2	299.4
2			272.8	307.4
3			304.8	268.2
4			304.1	267.5
5	0	98.1	273.4	308.8
6			270.3	306.8
7	39.2	39.2	272.0	306.1
8			270.3	299.1
9	39.2	98.1	268.1	297.9
10			270.4	304.9

Table 3 Experimental results of thermal contact resistance

Test case no.	Thermal resistance R_{io}, k/W	Resistance of conduction R_s, K/W	Contact resistance R_e, K/W
1	42.7	2.2	40.5
	42.7		40.5
2	44.6		42.4
	44.8		42.6
3	40.2		38.0
	40.4		38.2
4	40.2		38.0
	40.8		38.6
5	63.1	2.7	60.4
	65.2		62.5
6	62.4		59.7
	65.4		62.7
7	40.4	2.2	38.2
	41.6		39.4
8	41.1		38.9
	41.7		39.5
9	36.6	2.2	34.4
	38.2		36.0
10	37.1		34.9
	38.8		36.6

Comparison of Experimental Results with Predictions

The thermal contact resistance between the balls and the inner and outer rings was predicted taking into account the parameters of each test case. The thermal conductivity of 21.9 W/mK was taken as the property of SUS 440C at the mean temperature of 286 K.

Contact Resistance Under Axial Load

A comparison of the test results with the predicted contact resistances are shown in Table 4a. The maximum ratio of test result to predicted resistance was 1.07 for test case 2. This slightly large ratio might be due to the sensitivity of the test result to the temperatures of the shaft as described regarding the experimental uncertainty. However, the ratios of test re-

Table 4 Experimental results and predictions

Test case no.	Load, N Axial	Load, N Radial	Measured, K/W	Predicted, K/W
		a		
1	39.2	0	40.5 ± 0.0	39.5
2			42.5 ± 0.1	39.6
3			38.1 ± 0.1	36.6
4			38.3 ± 0.3	36.6
7	39.2	39.2	38.8 ± 0.6	37.3
8			39.2 ± 0.3	37.5
		b		
5	0	103.5	60.4	61.1
			62.5	62.6
6			59.7	61.2
			62.7	62.6
9	39.2	103.5	35.2 ± 0.8	35.1
10			35.8 ± 0.9	35.1

sults to predictions were less than 1.05 for test cases 1, 3, and 4. Therefore, it can be said from an engineering point of view that the macroscopic contact area calculated by using the Hertzian theory is sufficiently accurate to allow the prediction of contact resistance if the surface has a roughness less than 0.5×10^{-6} m.

Contact Resistance Under Radial Load

In test cases 4 and 5, the mass of shaft, 0.55 kg, acted upon the bearing in addition to the spring loading. The total radial load was thus taken as 103.5 N when predicting the contact resistance. Before and after the tests, the angle between the direction of the load and the line connecting the centers of the ball nearest it and the bearing was determined carefully, since the angle was required to calculate the contact force. The actual position, shown in Fig. 7, was maintained during the tests.

Based on the above discussion, it was considered that the resistance obtained from the temperatures measured at the positions near the load direction, i.e., the y axis in Fig. 7, approximated the value that would be obtained when the ball between the temperature measurement points coincided with the load direction. The test result was then considered to be equivalent to the resistance that was obtained by connecting the same three predicted values in parallel. For these cases, the contact force P_0 in the prediction was calculated by using $\theta = 0.898$ rad and Eq. (14a).

On the other hand, if it is assumed that the radial load direction passes through the center between two balls, the number of balls that concern the contact resistance becomes four, and their positions lie on the lines 4-1 and 4-2 shown in Fig. 7. Thus, it was considered that the test result obtained from the temperatures near the x axis approximated the resistance predicted for the ball located on line 4-2. Using $\theta = 0.898$ rad, contact force P_2 for the ball located on line 4-2 was calculated by Eqs. (15a) and (15b).

A comparison of the test results and the prediction values is given in Table 4b, and the agreement between both results is excellent. Therefore, we can say that the calculation method is applicable to the prediction of contact resistance between the elements of a bearing sustaining radial loads.

Contact Resistance Under Combined Load

The static equivalent loads for the bearing were given as follows:

$$F_e = 0.6F_r + 0.5F_a, \quad (F_r \leq 1.25F_a) \tag{22a}$$

$$F_e = F_r, \quad (F_r > 1.25F_a) \tag{22b}$$

According to these equations, the prediction for test cases 7 and 8 can be performed in the same manner as that for the axial load of $F_e = F_a = 46.9$ N, although cases 9 and 10 seem to be treated as the radial load of $F_e = F_r = 103.5$ N. However, cases 9 and 10 require careful consideration as to whether the included angle between the directions of the combined load and the radial load component is less than the contact angle of the bearing, because of the reason stated in the chapter regarding contact forces.

Cases 7 and 8: The contact resistance was predicted using the static equivalent axial load $F_e = 46.9$ N. The results of the tests and the predictions are shown in Table 4a, and it can be said that the agreement between both results is as excellent as in the cases of axial load only.

Cases 9 and 10: The included angle between the direction of the combined load and the radial load component was 0.362 rad. This angle was larger than the contact angle of 0.262 rad. Thus, it was considered that the four balls above the x axis were subjected to the axial load component with an angle of 0.362 rad, and the three balls below the x axis sustained a combined load acting in the direction of 0.362 rad. The total resistance was predicted by connecting each thermal resistance in parallel. A comparison of the test results with the predicted contact resistances is shown in Table 4b. The ratio of the test result to the predicted resistance was 1.0 and 1.02 for cases 9 and 10, respectively. Therefore, we can say that the proposed method for combined loading well-predicts the contact resistance between the bearing elements.

Concluding Remarks

A calculation method based on precisely determined contact forces has been presented to predict the thermal contact resistance between the balls and the inner and outer rings of a space-use dry bearing. The study assumed that a stationary ball bearing sustained axial, radial, or combined loads under a steady-state temperature condition. While the thermal analysis method is the same as that employed to determine constriction resistance, the assumptions commonly utilized in the constriction problem have been numerically confirmed to be applicable to the prediction of the contact resistance between the bearing elements. Also, the calculation of the contact resistance has indicated that the careful consideration of changes in the contact angle is important to determine the contact force and area due to the axial loads.

For the load types dealt with, limited test data were used to verify the proposed method because it was not easy to get the same temperature distribution across the bearing when the magnitude of load was changed, and the total number of operations had to be restricted to avoid changing the surface condition. However, it can be said that the excellent agreement between the test results and the predictions has confirmed the applicability of the proposed calculation method.

References

[1]Ohtomo, I., and Kumazawa, H., "Development of the On-Board Fixed and Mobile Multi-Beam Antenna for ETS-VI Satellite," *AIAA 13th International Communication Satellite Systems Conference*, AIAA, Washington, DC, 1990 (AIAA Paper 90-0805).

[2]Kawakami, Y., Hojo, H., and Ueba, M., "Design of an On-Board Antenna Pointing Control System for Communication Satellite," *AIAA/AAS Astrodynamics Conference*, AIAA, Washington, DC, 1988 (AIAA Paper 88-4306).

[3]Misawa, M., Yasaka, T., and Miyake, S., "Analytical and Experimental Investigation for Satellite Antenna Deployment Mechanisms," *Journal of Spacecraft and Rockets*, Vol. 26, No. 3, 1989, pp. 181–187.

[4]Tsunoda, H., Nakajima, K., and Miyasaka, A., "Thermal Design Verification of Large Deployable Antenna for ETS-VI," *Journal of Spacecraft and Rockets*, Vol. 29, No. 2, 1992, pp. 271–278.

[5]Yovanovich, M. M., "Thermal Constriction Resistance of Contacts on a Half-Space: Integral Formulation," AIAA Paper 75-708, 1975.

[6]Yovanovich, M. M., and Schneider, G. E., "Thermal Constriction Resistance Due to a Circular Annular Contact," AIAA Paper 76-142, 1976.

[7]Schneider, G. E., "Thermal Constriction Resistance Due to Arbitrary Contacts on a Half-Space—Numerical Solution of the Dirichlet Problem," AIAA Paper 78-870, 1978.

[8]Clausing, A. M., and Chao, B. T., "Thermal Contact Resistance in Vacuum Environment," *Transactions of the American Society of Mechanical Engineers*, Ser. C., Vol. 87, 1965, pp. 243–251.

[9]Madhusudana, C. V., and Fletcher, L. S., "Contact Heat Transfer—The Last Decade," *AIAA Journal*, Vol. 24, No. 3, 1986, pp. 510–523.

[10]Yovanovich, M. M., "Recent Development in Thermal Contact, Gap and Joint Conductance Theories and Experiment," *Proceedings of the 8th International Heat Transfer Conference* (San Francisco, CA), 1986, pp. 35–45.

[11]Yovanovich, M. M., "Thermal Contact Resistance Across Elastically Deformed Spheres," *Journal of Spacecraft and Rockets*, Vol. 4, No. 1, 1967, pp. 119–122.

[12]Yovanovich, M. M., "Thermal Constriction Resistance Between Contacting Metallic Paraboloids: Application to Instrument Bearings," AIAA Paper 70-857, 1970.

[13]Yovanovich, M. M., "Simplified Explicit Elasto-Constriction Resistance Expression for Ball/Race Contacts," AIAA Paper 78-084, 1978.

[14]Timoshenko, S., and Goodier, J. N., *Theory of Elasticity*, 2nd ed., McGraw-Hill, New York, 1951, Chap. 13.

[15]Love, A. E. H., *A Treatise on the Mathematical Theory of Elasticity*, 4th ed., Dover, New York, 1944, Chap. VIII.

[16]Seeley, F. B., and Smith, J. O., *Advanced Mechanics of Materials*, Wiley, New York, 1963, Chap. 11.

[17]Cooper, D. H., "Hertzian Contact-Stress Deformation Coefficients," *Journal of Applied Mechanics*, Vol. 36, June 1969, pp. 296–303.